A reliability-centered methodology for identifying renovation actions for improving resilience against heat waves in power distribution grids

Luca Bellani[a], Michele Compare[a], Enrico Zio[a,b,c,d], Alessandro Bosisio[c], Bartolomeo Greco[e,f], Gaetano Iannarelli[e,f], Andrea Morotti[e]

[a]*Aramis s.r.l., via G.B. Pergolesi 5, Milano, 20124, Italy*
[b]*Department of Energy, Politecnico di Milano, via La Masa 34/3, Milano, 20156, Italy*
[c]*MINES ParisTech, PSL Research University, CRC, BP 207, Sophia Antipolis Cedex, F-06904, France*
[d]*Eminent Scholar, Department of Nuclear Engineering, College of Engineering, Kyung Hee University, Republic of Korea*
[e]*UNARETI S.p.A., Corso di Porta Vittoria, 4, 20122, Milano, Italy*
[f]*Department of Astronautics, Electrical and Energy Engineering, Università degli Studi La Sapienza, Via Eudossiana, 18, 00184, Roma, Italy*

Abstract

In performance-based regulation paradigms, national authorities offer incentives to distribution system operators to develop plans for increasing the network resilience against natural hazards, such as heat waves, hurricanes, rain bombs, flooding. In this paper, we propose an approach, compliant with the Italian performance-based regulation framework, to prioritize renovation actions on sections of electrical power distribution networks for improving resilience against heat waves. The approach is made up of three steps, each addressed through a novel methodology: i) define the hazard of interest, i.e., heat waves; ii) estimate the reliability of the network branches; iii) prioritize the renovation interventions on the network to improve its resilience. The methodology has been applied to the medium voltage distribution network of Milano, Italy, yielding the identification of prioritized intervention actions to submit to the authority for incentives.

Keywords: Power distribution networks, Resilience, Heat Waves, Reliability of branches, Performance-Based Regulation, Accelerated Failure Time, Markov Chain, Logistic Regression.

1. Introduction

Reliability metrics such as Customer Average Interruption Duration Index (CAIDI), System Average Interruption Duration Index (SAIDI), System Average Interruption Frequency Index (SAIFI), Customer Average Interruption Frequency Index (CAIFI) and others, are widely adopted by Distribution System Operators (DSOs) for measuring the reliability of Electrical Power Distribution Networks (EPDNs) and demonstrating the capability of coping with power outages that occur under relatively normal conditions of operation [1].
These metrics, however, are not appropriate to assess the capacity of EPDNs of providing service continuity in case of extreme natural events, e.g., Heat Waves (HWs), earthquakes, hurricanes, flooding, etc., which force the network to operate beyond design conditions. Failures caused by these extreme events can lead to extensive and long-lasting interruptions, also in EPDNs serving large urban areas [2, 3, 4]. Accordingly, many national authorities, including the Italian Regulatory Authority for Energy, Networks and Environment (ARERA), have introduced the concept of resilience into their regulatory frameworks [5, 6].

1.1. Resilience of EPDNs

In the context of EPDNs, resilience refers to the ability of the network to continue operating and delivering power even when Low-Probability High-Consequence (LPHC) disruptions occur [7, 8]. Then, designing and managing for resilience aim at providing the EPDN with the capability of absorbing, recovering from and adapting to disruptions, to minimize their consequences [9].
Formal definitions, metrics and methods for analyzing and operationalizing grid resilience are currently being discussed and under development [10], also considering interdependent critical infrastructures [11]. For example, [12] presents a framework for evaluating power grid resilience based on a real blackout occurred in south Australia in 2016. In [13], a method is proposed to evaluate the resilience of EPDNs by focusing on the impact of critical loads under extreme weather events, whereas [14] presents a resilience-based framework for optimal switch placement in distribution systems. Concerning the hurricane natural hazard, a framework for evaluating the power system resilience is presented in [15], whereas a method to optimally allocate generation resources is proposed in [16]. A full-time scale resilience enhancement

framework against ice disasters is proposed in [17]. A quantitative framework for assessing resilience against extreme weather events is proposed in [18]. Finally, [19] investigates the impact of extreme HWs and drought events on the resilience of power grids fed by renewable energy systems.
At present, no grid resilience definition, metric or method of evaluation have received universal acceptance [1]. Nonetheless, incentives are offered to DSOs by national authorities to develop plans for increasing the network resilience, within Performance-Based Regulation (PBR) paradigms.

1.2. Performance-Based Regulation for resilience incentives

PBR is a regulatory framework to encourage, typically by explicit financial incentives, regulated companies such as utilities, to achieve pre-fixed performance goals [20]. A significant discretion is granted in developing the plans, to allow the companies to leverage their abundant knowledge of the operating environment for successfully achieving the goals.
PBR has become increasingly popular worldwide, yielding significant inroads in many regulated industries, including the energy industry [20], where regulators continuously share their regulatory structures in an effort to understand and compare the approaches of each other. As a consequence, the regulatory paradigms have increasingly converged, with a general growing emphasis in performance and quality of service [21]. Nonetheless, a variety of regulatory models will continue to coexist in the short term future ([21]), which limit the applicability of any method to improve network resilience to the PBR framework it has been devised for, unless it is opportunely customized. Obviously, this does not diminish the value of the research in the field. Rather, the larger the number and variety of proposed approaches, the more informed is the path to converge towards a common basis.
In Italy, ARERA issued the national PBR approach, resolution 668/2018/R/eel [22], which builds on i) the concept that interruptions due to extreme events have to be quantitatively measured by network resilience metrics, rather than reliability metrics: ii) the approach of giving incentives to DSOs for strengthening the power supply continuity performance in case of natural hazards. To apply for obtaining the incentives, DSOs have to prepare a three-year plan for implementing these actions.
Depending on the territory where the DSOs operate, the main natural hazards to be considered are:

- HWs and long periods of drought;

- Intense snowfalls, causing the formation of ice or snow sleeves wet snow [23];
- Floodings due to intense rainfall;
- Wind storms and effects of salt pollution nearby the seaside;
- Fall of trees on overhead lines.

1.3. Context, objectives and novelty of the work

We consider the EPDN of Milano (Italy), consisting of about 600 Medium Voltage (MV) feeders at 23 kV, and about 880'000 Low Voltage (LV) customers served by more than 6'000 MV/LV substations.
In this specific case, HWs are the main natural hazard to be considered to prepare the resilience plan compliant with the PBR approach. Indeed, HWs have affected almost 1 million people in the last 10 years, whereas, for comparison, flooding, the second most relevant hazard, has affected "only" 70'000 customers in the same period [24]. Moreover, in the forthcoming years climate change is expected to make HWs more intense and frequent than before.
The proposed framework is based on the following steps, each addressed through a dedicated innovative approach:

1. ***HWs definition.*** To set the PBR incentive policy and develop valuable resilience plans, a clear definition is needed of the extreme events that determine the "beyond design" conditions, which shift the focus from reliability to resilience. At present, this definition is lacking for HWs. The novelty of the contribution lies in that we propose to frame the HWs definition as a supervised classification problem, addressed by the logistic regression algorithm [25, 26].
2. ***Characterization of the reliability of the network branches.*** We develop an Accelerated Failure Time (AFT) model [27], which encodes the main covariates influencing the reliability behavior of the network branches, i.e., network arcs from substation to substation. The approach is novel in that it allows estimating the reliability of long-time operated networks, which are characterized by lack of registry data, inhomogeneity of component materials and technologies, and variability of operation settings.

3. ***Prioritization of the renovation interventions.*** The novel contribution of the approach devised to address this step is the combination of a Shortest Path Problem (SPP)-based algorithm [28], to identify specific portions of the network, with Markov chain [29] modeling, to provide a quantitative basis to identify the portions for which renovation actions bring the largest benefit to network resilience.

Overall, the full-fledged approach proposed to prepare a plan compliant with the PBR framework is a furher novelty of the contribution.
The remainder of the paper is as follows. In Section 2, we propose an approach for the quantitative definition of HWs. In Section 3, we develop a reliability model for the branches of the network. In Section 4, we develop the approach to identify the renovation actions to take for increasing the EPDN resilience. In Section 5, the presented framework is applied to the EPDN of Milano, Italy. In Section 6, conclusions are drawn.

2. Heat waves definition

HWs are due to extremely hot weather conditions, and result in both the reduction of the heat transfer from cables to soil and the increase of power demand caused by the massive and simultaneous use of air conditioning. When these conditions last for some days, the network cables can reach high temperatures, even 30°C larger than in the winter season, with consequent heavy thermal stresses causing multiple failures. Additional details on the impacts of rising ambient air temperatures on electric transmission ampacity and peak per-capita can be found in [30], whereas the impact of HWs on the energy systems is analyzed in [31] from a more general perspective.
We propose a data-driven framework for the quantitative definition of HWs. The same issue is tackled in [32] with an unsupervised Gaussian mixture clustering approach [33, 34]. The method is applied to temperature and relative humidity data collected in Torino, Italy, over a period of 10 years. The framework proposed in [32] suffers from the following limitations:

- the unsupervised framework allows characterizing the different climate conditions, but these are not directly linked to the failures occurred, i.e., the information about the failures is not fully exploited;
- from the analysis of the results reported in [32], it emerges that the unsupervised framework is not capable of properly isolating the HW

periods. Rather, it separates the summer period from the rest of the year: almost 35% of the yearly data is included in the cluster with large temperature and small humidity values. The proportion of days associated to large temperature values, more than one third, is too large to be a proper indicator of HWs. It cannot be considered as an extreme event, i.e., LPHC disruption;

- no account is given to the loading conditions of the network, although it is known that they strongly affect the cables temperature and, thus, their failure behavior.

To advance on these issues, we resort to supervised classification, which means learning a function that maps input data onto an output class, based on example input-output pairs (e.g., [26, 35]). Although there are plenty of algorithms for supervised classification (e.g., [36]), to the best of the authors' knowledge the proposed approach is novel with respect to those already available in the literature, as it uses supervised learning to systematically define HWs by creating a quantitative association between failure data and environmental and operating conditions of the EPDN.
We consider HWs as those periods in which the weather and operating conditions of the network are such to determine failure occurrence behaviors statistically different from those of other periods, which are considered of normal failure behavior. To translate this intuitive concept into a quantitative definition, we relate the number of occurred failures to weather conditions and network loads. Specifically, we consider the following data, limited to M days of the period May-September and recorded for Y years:

- total daily load of the electricity network. In the case of Milano, these are sampled every 15 minutes at the HV/MV transformers;

- temperature and relative humidity. For the Milano case study, these data are collected from weather stations every 10 minutes;

- failure data. These are relevant to cables and joints, only. Thus, we do not consider substation failures, as these are typically not associated with HWs. Yet, we consider only the failures whose causes are not associated with others hazards, e.g., floods. We define $\phi(t)$ as the variable which counts the number of simultaneous failures at time step t. The data encode the timestamps of the failures.

We define the HW period of Δ days in which more than F failures occur. $F \in [F_{min}, F_{max}]$ is the discriminating threshold to be identified for distinguishing between normal and HW conditions, with respect to failure occurrence. The values F_{min} and F_{max} are selected by an Inter Quartile Range (IQR)-based outlier detection procedure [37], setting F_{min} as 3-rd quartile + $1.5 \cdot IQR$ and F_{min} as 3-rd quartile + $4 \cdot IQR$.
The samples of Y years recordings are appended one after the other, so that the complete dataset includes $D = \lfloor \frac{M}{\Delta} \rfloor \cdot Y$ samples, where $\lfloor \square \rfloor$ denotes the integer part of its argument. The timestamps of the Δ-length windows are given by Eq. 1, where $t_{\delta,y}$ identifies the date of the δ-th sample of year $y \in \{1, ..., Y\}$ and $t_{0,y}$ is pre-fixed for all the years considered. Notice that, for simplicity, in Eq. 1 we assume that $\frac{M}{\Delta} > \lfloor \frac{M}{\Delta} \rfloor$.
Formally, label $y_d = 1$ identifies the HW in the dataset as the Δ days corresponding to period $\mathcal{T}_d = [t_d - \Delta, t_d]$ in which at least F failures have occurred, $d \in \{1, \ldots, D\}$; $y_d = 0$ is the label assigned to the opposite case.

$$\begin{aligned} t_d &= t_{\delta,y} + \Delta \\ \delta &= (d-1) \mod \left\lfloor \frac{M}{\Delta} \right\rfloor \\ y &= \left\lfloor \frac{d \cdot \Delta}{M} \right\rfloor + 1 \\ d &= 1, ..., D \end{aligned} \tag{1}$$

To identify the conditions that define the HW occurrence, we extract I features from the load, temperature and humidity data, including maximum, minimum, average, standard deviation, skewness and kurtosis, each calculated on W different time windows, i.e., 3 days, 5 days, 7 days, 10 days, 15 days, 20 days. These feature values are arranged in vector $\mathbf{z}_d \in \mathbb{R}^{I \cdot W}$, $d \in \{1, \ldots, D\}$. We then build a classifier function $\hat{y} = f(\mathbf{z})$ mapping the generic vector of environmental and operating condition features $\mathbf{z}$, onto the indicator of HW occurrence.
For supervised classification, we rely on a binary logistic regression classifier with elastic-net penalties to automatically select the features of interest among those $I \cdot W$ considered [25, 26]. The logistic regression problem reads as in Eqs. 3-6. Namely, the logistic regression in Eq. 3 provides the probability $\mathbb{P}(\hat{y} = 1|\mathbf{z})$ that the prediction $\hat{y}$ is equal to 1, depending on the features

values $\mathbf{z}$ and the corresponding coefficients $\boldsymbol{\alpha}$. Once the logistic regression classifier is trained, we can set prediction $\hat{y} = 1$ (HW occurs) if and only if $p_{\boldsymbol{\alpha}}(\mathbf{z}) \geq 0.5$. The probability value $p_{\boldsymbol{\alpha}}(\mathbf{z})$ can be regarded as the degree of confidence in our prediction $\hat{y}$, in this case beyond coin-flipping random prediction.
With respect to Eq. 5, two issues must be considered when building a classifier of HWs:

- the two classes of HWs and normal conditions are unbalanced: the HW periods are far fewer than the normal conditions ones, i.e., $\sum_{d=1}^{D}(1 - y_d) >> \sum_{d=1}^{D}(y_d)$. Then, considering the overall accuracy of the classification as loss function may lead the classifier not to successfully identify the class of interest, $y_d = 1$;

- to be conservative, it is more important to limit the number of False Negatives (FNs), i.e., observations for which $y_d = 1$ and $\hat{y}_d = 0$, than the number of False Positives (FPs), i.e., observations for which $y_d = 0$ and $\hat{y}_d = 1$, $d \in \{1, \ldots, D\}$. Indeed, rather than not triggering alarms when the HW risk is high, it is preferable to warn of the risk of an anomalous number of them, even if it is not true that they have occurred. This is in agreement with our definition of HWs: even if the considered dataset contains multiple periods of hot weather conditions, these are not necessarily associated to large numbers of failures.

To address these issues, in Eq. 5 we impose that in the training phase the weight of the FNs error is $E = 20$ times that associated with the FP error. Coefficients ω_1 and ω_2 of the ℓ_1 and ℓ_2 penalization values, e.g., [26], in Eq. 4 are chosen by $C-$fold cross-validation, combined with threshold F optimization [38]. Thus, the available dataset $\mathcal{F}$ is partitioned into C folds containing time windows of equal duration. Set $\mathcal{F}_c \subset \{1, ..., D\}$ contains the $\underline{D} = \left\lfloor \frac{M}{\Delta} \right\rfloor$ indexes of the data in the c-th fold, $c = 1, ..., C$. We solve the classification problems $\mathcal{C}_c$ by training the algorithm on $C-1$ folds, containing the $\overline{D} = \left\lfloor \frac{M}{\Delta} \right\rfloor \cdot (Y - 1)$ data $[\mathbf{z}_{\overline{d}}, y_{\overline{d}}]$ such that $\overline{d} \in \{1, ..., D\} \setminus \mathcal{F}_c$, and testing the accuracy of the classification on data $[\mathbf{z}_{\underline{d}}, y_{\underline{d}}]$, $\underline{d} \in \mathcal{F}_c$. The procedure is repeated on all C folds. Finally, we select the penalization parameters, the threshold F_c^* and $\boldsymbol{\alpha}_c^*$ of the classification problem with the largest Balanced

Accuracy (BA) shown in Eq. 2:

$$\mathrm{BA}(\mathcal{C}_c) = \frac{\frac{\sum_{\underline{d}=1}^{D} y_{\underline{d}} \cdot \hat{y}_{\underline{d}}}{\sum_{\underline{d}=1}^{D} y_{\underline{d}}} + \frac{\sum_{\underline{d}=1}^{D} (1-y_{\underline{d}}) \cdot (1-\hat{y}_{\underline{d}})}{\sum_{\underline{d}=1}^{D} (1-y_{\underline{d}})}}{2} \tag{2}$$

$$\mathbb{P}(y=1|\mathbf{z}) = p_{\boldsymbol{\alpha}}(\mathbf{z}) = \frac{1}{1+e^{-\boldsymbol{\alpha}\cdot\mathbf{z}}} \tag{3}$$

$$\boldsymbol{\alpha}_c^* = \underset{\boldsymbol{\alpha}_c \in \mathbb{R}^{I\cdot W}}{\arg\min} \frac{1}{\overline{D}} \sum_{\overline{d}=1}^{\overline{D}} k(\mathbf{z}_{\overline{d}}, y_{\overline{d}}) + \frac{\omega_1}{I\cdot W} \sum_{i=1}^{I\cdot W} |\alpha_{c,i}| + \frac{\omega_2}{2\cdot I\cdot W} \sum_{i=1}^{I\cdot W} \alpha_{c,i}^2 \tag{4}$$

$$k(\mathbf{z}_{\overline{d}}, y_{\overline{d}}) = -\frac{E}{E+1} \cdot y_{\overline{d}} \cdot \log(p_{\boldsymbol{\alpha}_c}(\mathbf{z}_{\overline{d}})) - \frac{1}{E+1} \cdot (1-y_{\overline{d}}) \cdot \log(1-p_{\boldsymbol{\alpha}_c}(\mathbf{z}_{\overline{d}})) \tag{5}$$

$$y_d = 1 \quad \Longleftrightarrow \int_{t_{d-1}}^{t_d} \phi(t)dt > F^* \tag{6}$$

The optimized parameters $\boldsymbol{\alpha}_c^*$ characterize the relative importance of the various features, i.e., $\alpha_{c,i}^*$ represents the contribution of feature $z_{d,i}$ to defining output $\hat{y}_d$. Notice that the penalization parameters ω_1 and ω_2 may set some coefficients to 0. This allows performing feature selection directly in the training phase: $\alpha_i^* = 0$ indicates that feature $z_{d,i}$ has no significant impact on $\hat{y}_d, d \in \{1,\ldots,D\}, i \in \{1,\ldots,I\cdot W\}$.

Notice also that the optimization of F entails that the HW is defined by the set of environmental and operating conditions, which allow fixing a threshold on the number of failures that best distinguishes the HWs from the normal conditions.

Finally, the choice of relying on logistic regression rather than on other supervised classification algorithms is twofold. On the one hand, logistic regression with penalization does not suffer from the curse of dimensionality like other algorithms, e.g., K-nearest-neighbour [39], and generally provides good classification results and features selection when trained with a large number of features. On the other hand, unlike support vector machines [40], random forests [41], neural networks [42], it has a faster training phase and provides results that are easy to interpret by experts.

3. Characterization of the network branches reliability

Once the HW conditions are identified, we have to characterize the reliability of the network components under these stressing conditions. This issue is very challenging in practical applications, due to the following main reasons:

- in case of failure, usually only the failed part is repaired. On the one hand, this restoration policy allows DSOs to extend the life of the cables beyond the manufacturers' recommended lifetime [43], while limiting the maintenance costs and avoiding the setting up of large construction sites for digging. On the other hand, it makes the branches of the networks with long operational history, as in the case of Milano, extremely inhomogeneous: the situation typically encountered is that a branch is made up of portions of cables of different lengths, diverse insulation and conductor materials, connected by joints of very different technologies;

- the electrical networks are extremely dynamic systems: both their topological and operating configurations change in time. This makes the stressing conditions very variable and difficult to be traced over long time horizons [44];

- the very long operating time of the networks of many large cities, including Milano, makes the knowledge of the network characteristics and history incomplete: a significant part of the network was installed or repaired before the advent of digitization, whereby the corresponding information is often missing in the databases.

- Failure data mostly relate to normal operating conditions, rather than HWs.

Different models have been proposed to estimate the reliability of electrical components, also considering the effect of the influencing factors, e.g., [43], [45], [46]. However, these models require the knowledge of the whole operating profile of each network part, from its laying date, and homogeneity of part characteristics. As mentioned before, these data are usually lacking for aged networks.
To give due account to all these issues and fully exploit the available limited

knowledge, we propose a novel AFT reliability model at branch level, considering the known available characteristics as covariates [27].
Formally, the network is made up of branches $b \in \{1, ..., B\}$, whose reliability depends on relevant covariates $f_{i,b}$, $i \in \{1, ..., N\}$. The failure rate λ_b of branch b reads as in Eq. 7 :

$$\lambda_b\left(t|f_{1,b}, ..., f_{N,b}\right) = \lambda_0 \cdot e^{-\sum_{i=1}^{N} \beta_i \cdot f_{i,b} - \beta^* I_h(t)} \tag{7}$$

where λ_0 is the base failure rate; β_i, $i = 1, ..., N$, are the weights associated with the selected covariates, which can accelerate or decelerate the degradation process; $I_h(t)$ is the HW indicator. This latter is set to 1 in case of HWs and 0 otherwise. β^* sets the increment of failure rate during the HW.
Notice that considering $I_h(t)$ as a covariate allows using failure data in both HW and not HW conditions to infer the model parameters.
The set of covariates relevant to predict the component reliability is selected from those derived from the available data. In the case of the MV network of Milano, the following are considered:

- cable characteristics. We consider the insulator material, i.e., cross-linked polyethylene (XLPE), different types of rubbers and papers [43], and the conductor material, i.e., aluminium and copper [47]. For each branch, we know the length and position of each piece of cable, whose edges terminate either in joints or in links to the substations or busbars. The laying date of most of the cable portions is unknown;

- joint characteristics. Joints are of different technologies, developed over the years, and are normally the weakest parts of the branch [48]. For each branch, we know the exact number and position of joints. The laying date of most of the joints is unknown;

- past failure events on busbars and feeders, i.e., sequences of branches starting from the High Voltage (HV) busbars. This factor can be relevant because the overcurrents originated by the failure of one branch of a feeder accelerate the degradation of the upstream branches. Notice that the exact number of overcurrent events experienced by each branch is unknown, as this would require tracking the branch position with respect to the failure through the entire lifetime, which is very challenging due to the variability of the network configuration. To sidestep this issue, we assume that the effects of an overcurrent can

be estimated as if the actual network configuration were the same as in the past. Indeed, the information we want the model to capture is that the first branches of the feeder are overstressed and, thus, more prone to fail if they have already failed: whichever the actual network configuration was when the failure occurred, the first branches of the current feeders are likely to have been the first also in the past;

- current load on the branches, obtained through a power flow model. The value considered is static: it refers to a specific time instant, which is the load peak in the last year. This pointwise load value can be interpreted as the load distribution among the various sections. This is an over-simplifying assumption, which is necessary because considering the load variation over long periods would require very long computational times. This issue will be tackled in future research work, e.g., following [49, 50].

Based on the aforementioned information, we have derived $N >> 1$ covariates such as the total length of each insulator material, its percentage with respect to the branch, the total number of joints, also divided by the cable length, the number of joints connecting two different insulators, etc.
The model parameters are maximum-likelihood estimated, by considering for each branch $b \in \{1, ..., B\}$ with known covariates $f_{i,b}$, $i = 1, ..., N$, both the failure times and the righ-censoring time at the end of the observation window [2]. Namely, each branch has at least one associated event:

- censoring time at the observation period. In case the branch had no failures, which applies to the vast majority of branches, the censoring interval starts at the beginning of the observation period; otherwise, it starts from the last failure;

- the failure times.

Thus, we have a set of $G \geq B$ times $t_1, t_2, ..., t_G$, each associated to the characteristics of the branch and to the binary flag $\xi_1, \xi_2, ..., \xi_G$ indicating whether the time refers to a failure or to survival until the end of the observation window.
To eliminate the less influencing covariates, we have used the backward elimination technique, with different threshold values for the p-value [51]. Then, we have selected the model with the covariates yielding the best Akaike Information Criterion (AIC) value [52].

It is worth concluding this Section with some comments about the assumptions underlying the model in Eq. 7:

- the failure behavior of the single branch, inferred from a Y-year time window, obeys the exponential distribution, with the memoryless property. This assumption is not very limiting if we use the reliability model for short-term predictions, as in the case of resilience plans. Indeed, the increase of the failure rate due to wear out is not expected to be very fast. Moreover, we still consider the degradation due to aging: the covariates describing the characteristics of cables and joints depend on their age.

- the failure rate is different in HW and out-of-wave periods. Therefore, if we want to apply the model in Eq. 7 over time windows longer than the HW period, the failure rate is stepwise constant. Yet, the assumption that the yearly average of HWs frequency is constant entails that the memoryless assumption is still satisfied: a more rigorous approach will be developed in future research work, e.g., building on [53];

- we assume that the branch characteristics have remained constant over the Y-year period. While not satisfied, this assumption is still acceptable if Y is sufficiently short: given the size of the network, changes in the short-term past concern only a small portion of the network. Moreover, we favour covariates that are not sensitive to the small modifications of the network;

- the covariates are normalized. This implies that we are interested in their relative values, i.e., with respect to those of the other branches, rather than to their absolute values.

4. Prioritization of interventions for resilience improvement

The Italian PBR framework for resilience incentivizes the renovation actions that in case of hazardous conditions, e.g., HWs, prevent the long customer disconnections that occur with frequency larger than $1/50y^{-1}$. In this Section, we develop an approach to identify the network sections concerned with these events, which, in agreement with the PBR rationale, are the sections that contribute the most to the occurrence of failures entailing long

disconnections. Then, the interventions to reduce their failure rates are expected to bring the largest increase in network resilience.
Notice that the reference PBR framework does not consider the number of customers disconnected in case of failure. However, this criterion can be considered to prioritize the renovation actions of the network sections fulfilling the $1/50y^{-1}$ frequency threshold.
The analysis focuses on the MV feeders, which are the weakest part of the Milano EPDN: almost 80% of the recorded failures affect MV feeders, whereas only a few failures are experienced by HV/MV substations or by the LV distribution network [54].
As in many large cities, the MV network of Milano is topologically meshed so that when a branch fails, the network operating layout can be rapidly changed to guarantee the supply to the interrupted customers through another feeder. However, there can be double-failure events, like that schematized in Figure 1, which do not allow network re-configurations for supplying all customers. Differently for reliability, resilience is concerned with these double failure events, as they cause long interruptions.
Notice that one main assumption here is that the network cables are always available for switching during re-configuration. This is realistic for EPDNs serving large cities, whose cables are usually operated at a relatively small percentage (i.e., almost 40% for Milano) of the maximum current load, and whose substations are all equipped with switching capabilities. Moreover, we must bear in mind that final aim of the proposed methodology is to support decision making for planning interventions to improve the network resilience, whereby temporary conditions in which switching is not possible do not affect the generality of the approach.

Assume that the first failure occurs on the branch outgoing from vertex 1, i.e., the first part of the feeder. This is in agreement with the experience that failures are more likely to occur on these parts of the grid, loaded with the whole power delivered by the feeder. In case of an outage in vertex 1, an alternative path is needed to supply the red subsection: the first branch of the feeder from vertex 4 to vertex 2 has now to carry the whole power of the subnetwork highlighted in red. If a second failure occurs on the most loaded part of the network, i.e., close to 4, all the MV/LV substations in red remain not supplied until one of the two paths is repaired by field operators. The red subnetwork is defined as section and indicated by Γ. This situation is very critical in the case of underground cables, because the time to find and repair the outage can be long.

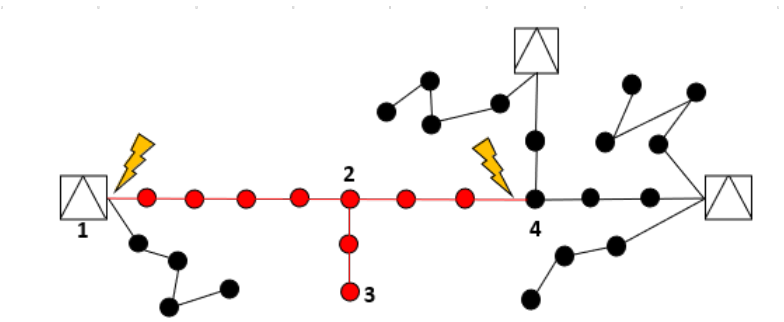

Figure 1: Double-failure event and MV/LV affected by power outage.

On this basis, to develop the plan to improve resilience against HWs, we first develop a novel algorithm to identify all the Γ sections $\gamma_1, ..., \gamma_\Gamma$ of the network exposed to potential double-failure events, as the red one shown in Figure 1. The arcs of γ_j are $\{s_{j,1}, ..., s_{j,S_j}\} \subset \{1, ..., B\}$, $S_j = |\gamma_j|$, $j = 1, ..., \Gamma$. Algorithm 1 in Appendix provides the pseudo-code to identify the Γ sections. Then, we estimate the probability of occurrence of a double-failure event for each section, based on the estimates of the failure rates of the individual branches. For this, we rely on a continuous time multi-state Markov model [29].

Practically, the resilience of these sections can be increased through two main actions: replacement of weak cables and increasing of meshing. In the former case, we aim at reducing the probability of occurrence of the first failure event, whereas in the latter at improving the restoration of the power supply in the section upon the first failure occurrence, by laying a new connection to another feeder. An example of this latter action is shown in Figure 2: it does not change the probability of a single failure, but the probability of double-failure events decreases when a new connection is built, as the set of possible additional failures that can disconnect customers in the new configuration is reduced [55].

4.1. Markov model for double-failure events occurrence probability estimation

To develop the Markov model, we make the following assumptions:

- we consider the HW periods only. Thus, $\lambda_b\left(t|f_{1,b}, ..., f_{N,b}\right) = \lambda_b^h = \lambda_0 \cdot e^{-\sum_{i=1}^{N} \beta \cdot f_{i,b} - \beta^*}$ is constant;
- the effects of the failure of one branch on the reliability of the other branches is negligible, although it generally results in a load increase.

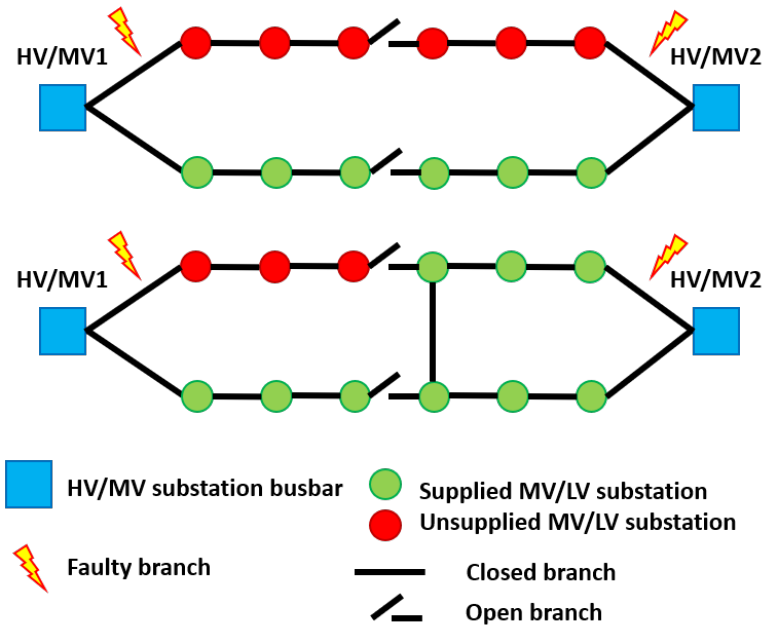

Figure 2: Action to improve network resilience. Top: initial section setting. Bottom: proposed intervention for improving resilience.

This assumption is due to the lack of data to quantitatively characterize this effect and the unfeasible computational burden required to consider all possible failures;

- the repair time obeys an exponential distribution, with rate μ_m.

Under these assumptions, we can define the $S_j + 2$ model states for sub-network γ_j as:

- state 0: all branches of γ_j are working;
- state $i = 1, ..., S_j$: only the i-th branch $s_{j,i}$ in γ_j is failed;
- state $S_j + 1$: there are two failed branches.

The goal is to estimate the time at which the system enters the absorbing failed state $S_j + 1$ for the first time. This is derived analytically by [29]:

- considering $\mathbf{Q_j}^*$ as the matrix obtained from the transition matrix $\mathbf{Q_j}$, Equation (6), by removing the absorbing state, i.e., last row and last column;

- solving the linear problem $\mathbf{xQ_j \cdot Q_j}^* = [1, 0, ..., 0]$, where $\mathbf{x} = [x_1, ..., x_{S_j+1}]$ is the vector containing the sojourn times in the different states.
- computing the rate of occurrence of the double-failure event as $\left(\sum_{i=0}^{S_j} x_i\right)^{-1}$.

$$Q_j = \begin{pmatrix} -\sum_{s=1}^{S_j} \lambda_{s_{j,s}} & \lambda_{s_{j,1}} & \dots & \lambda_{s_{j,i}} & \dots & \lambda_{s_{j,S_j}} & 0 \\ \mu_{s_{j,1}} & -\left(\mu_{s_{j,1}} + \sum_{s\in\{2,\dots,S_j\}} \lambda_{s_{j,s}}\right) & \dots & 0 & 0 & 0 & \sum_{s\in\{2,\dots,S_j\}} \lambda_{s_{j,s}} \\ \dots & \dots & \dots & \dots & \dots & \dots & \dots \\ \mu_{s_{j,i}} & 0 & \dots & -\left(\mu_{s_{j,i}} + \sum_{s\in\{1,\dots,S_j\},s\neq i} \lambda_{s_{j,s}}\right) & \dots & 0 & \sum_{s\in\{1,\dots,S_j\},s\neq i} \lambda_{s_{j,s}}) \\ \dots & \dots & \dots & \dots & \dots & \dots & \dots \\ \mu_{s_{j,S_j}} & 0 & \dots & 0 & \dots & -\left(\mu_{S_j} + \sum_{s\in\{1,\dots,S_j-1\}} \lambda_{s_{j,s}}\right) & \sum_{s\in\{1,\dots,S_j-1\}} \lambda_{s_{j,s}}) \\ 0 & 0 & \dots & 0 & \dots & 0 & 0 \end{pmatrix}$$

(8)

5. Results

This Section reports the results of applying the proposed methodology to the Milano MV distribution network and discusses the related findings.

5.1. Heat waves

We have considered $M = 153$, days in the period May-September and $Y = 5$ years. For cross validation, $C = 5$, each fold containing the data of one year.
Figure 3 reports the cumulative failures over $\Delta = 3$ days, i.e., $D = \frac{Y \cdot M}{\Delta} = 255$, for the distribution network of Milano, together with some features selected from those $I \cdot W = 144$ features extracted from temperature, load and relative humidity data.
For both confidentiality and visualization, features and failures have been re-scaled. Thus, the y-axis is quantitatively meaningless and we can only infer the relationships among these variables. From Figure 3, we can see that there is a strong correlation between the failure data and the environmental and operating conditions, especially with the maximum load over three days: the periods in 2015 and 2019 with the largest numbers of failures are in perfect correspondence with the load peaks. There is a positive correlation between the number of failures and the load and temperature data, whereas the correlation is negative between the failures and the relative humidity; smaller values of humidity generally correspond to fewer rainy days in the considered period.

The 10 features selected by the best setting of penalized logistic regression, i.e., leading to largest BA of Eq. 2 over the cross-validation and threshold-F possible combinations, are shown in Figure 4: the y-axis reports the feature coefficients $\boldsymbol{\alpha}$. Eight statistical features, i.e., skewness of humidity in 10 days, standard deviation of load over $3, 5, 7$ days, standard deviation of temperature over 20 days, mean of load over $3, 5$ days and maximum load over 3 days, have a positive value of the associated coefficient, which indicates that an increase in one of these features results in an increase of the probability of HW conditions. The remaining two features, i.e., maximum of humidity over 7 days and skewness of temperature over 5 days, have negative coefficients, which indicates that an increase in their value decreases the probability of having a HW. As already pointed out, a small value of maximum relative humidity over 7 days is generally associated

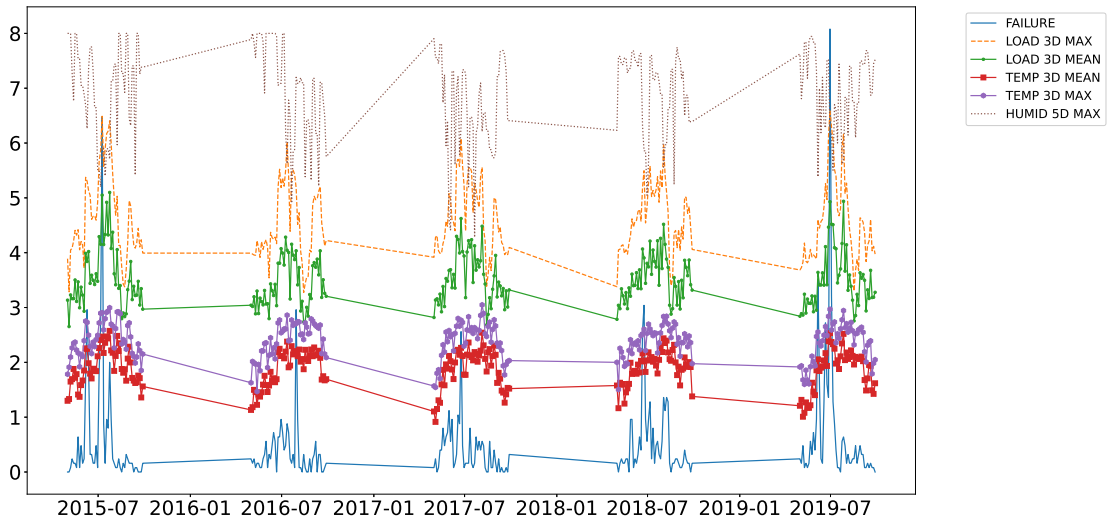

Figure 3: Number of Failures in 3 days and some features extracted from temperature, load and humidity.

to a sunny week; the skewness of the temperature is an indicator of the presence of sudden steps in the temperature value. It is worth noticing that the negative coefficient sign indicates that there is a larger chance of HW when, in a time window, there is a small proportion of measurements with small temperature values (negative skewness). The ten features selected seem in accordance with the literature, e.g., [56]. With respect to [32], it emerges that:

- in both approaches, large temperature and small humidity values are proper indicators of the heat conditions;
- the features related to the load, which have not been considered in [32], are those which mostly affect the number of failures, 6 out of 10, as the load directly affects the thermal stress on the cables;
- some features are not related to the absolute value of the environmental and operational conditions; rather, they are related to the presence of sudden changes, e.g., skewness of temperature, or total variation, e.g., standard deviation of load and temperature.

Notice that since the features have been normalized by z-score [39], the values of the coefficients can be somehow interpreted as the relative importance of

the features.

The 5− fold cross-validation performance of the algorithm is reported in

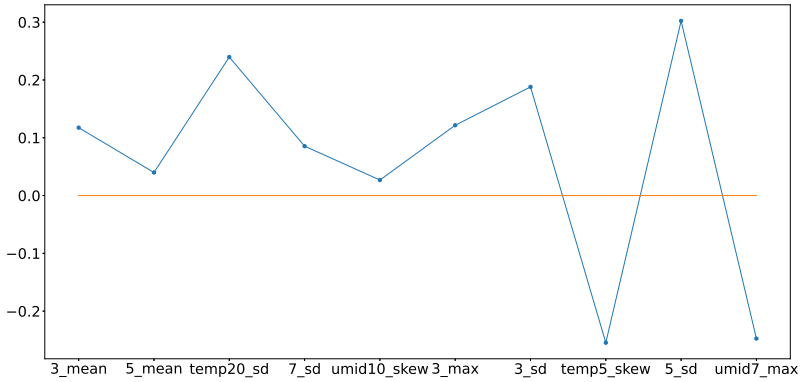

Figure 4: Value of the coefficient β_i^* for the 10 features selected by the elastic-net logistic regression. When we report only the time window in the x-axis, we refer to a feature extracted from the load, e.g., 3_mean stands for mean load over 3 days.

Table 1, where for each year the total numbers of True Positives (TPs), True Negatives (TNs), FNs and FPs and the corresponding Rates $TPR = \frac{TP}{TP+FN}$, $TNR = \frac{TN}{TN+FP}$, $FNR = \frac{FN}{TP+FN}$ and $FPR = \frac{FP}{FP+TN}$ are reported for all the 3− day periods considered. From the Table 1, it can be noted that there are only nine periods, sum of columns 2 and 4, in which more than F failures have been experienced. For confidentiality reasons, we cannot provide the value of F. Eight out of the nine periods have been properly identified by the algorithm. The only exception is for 2016, where the abnormal number of failures does not seem related to the environmental conditions: from Figure 3, it can be seen that the peak of failures occurs in a period with a relatively small load. Despite the apparently large number of FPs, columns 3 and 7, the total number of days considered by the algorithm as HWs, $\hat{y}_d = 1$, sum of columns 2 and 4, is in accordance with the environmental conditions of Milano: years 2015 and 2019, with 11 and 8 HW periods, respectively, have been among the hottest summers ever [57].

Moreover, 2015 is characterized by many temperature fluctuations, which are considered risky by the skewness of the feature temperature. On the other hand, 2016 has been one of the few years in the third millennium with a summer not characterized by extremely hot days [57] and the algorithm recognized only 4 HW periods.

With respect to the FP metric, we can also see that in spite of the 7 HWs identified sor 2017 by the algorithm, Figure 3 shows no days with peaks of failures, although the total number of failures occurred in 2017 is far larger than that in 2016. This is in agreement with the fact that the HW does not necessarily provide an abnormal number of failures, but does increase their probability.
Finally, it is worth noticing that the number of periods with HWs identified by the algorithm is 35, sum of columns 2 and 3, with $S \cdot 35 = 105$ days of HW in 5 years. Very roughly, we can estimate that the average frequency of extreme hot weather events is 21 days/year.

Table 1: "Confusion matrix" of the Proposed algorithm cross-validation performance; each fold corresponds to a different year.

Year	TP	FP	FN	TN	TPR	FPR	FNR	TNR
2015	3	8	0	40	1	0.17	0	0.83
2016	0	4	1	46	0	0.08	1	0.92
2017	0	7	0	44	N.A.	0.14	N.A.	0.86
2018	1	4	0	46	1	0.08	0	0.92
2019	4	4	0	43	1	0.09	0	0.91

5.2. Reliability model

The application of the methodology described in Section 3 has led to the selection of the following $N = 3$ covariates: the number of failures on the same primary substation, the number of joints connecting cables with the same insulation material and the number of joints linking cables with different insulation materials, i.e., XLPE-paper, paper-rubber, rubber-XLPE. Figure 5 shows the estimated values of the model parameters λ_0, β_i, $i \in \{1, ...3\}$ and β^*, with corresponding 95% confidence interval. For confidentiality, the scale of the Y-axis is not reported.
The features are not very sensitive to the network changes upon corrective maintenance. Indeed, considering that the features are normalized, we do not expect that the changes on a short Y-year period, i.e., installation of one or two joints and modification of the cable insulator material for a small portion of the branch, can modify the feature distributions.
Notice also that $\lambda_b^h = e^{-\beta^*} \cdot \lambda_0 \cdot e^{-\sum_{i=1}^{3} \beta \cdot f_{i,b}}$, where $e^{-\beta^*} \simeq 7.5$. Thus, on average, during the HW, we expect 7.5 times the failures during normal operation.

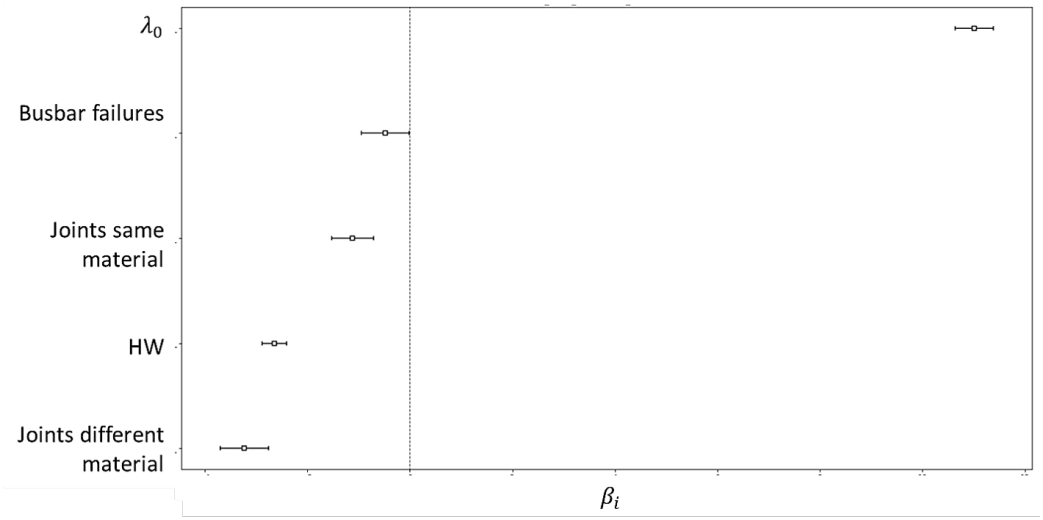

Figure 5: β factors value of the most influencing covariates, with corresponding 95% confidence interval.

To validate the model, we have considered the calculation of the Concordance Index (CI) on the test set, within a cross-validation scheme [58]. However, the CI and other similar metrics are hardly applicable to this case study, due to the very large censoring [59]. The development of dedicated metrics will be the focus of future research work.
To qualitatively demonstrate the effectiveness of the algorithm in identifying the correct ranking of the reliability of the network branches, their failures registered over the Y-year period are ordered by increasing failure rate ans shown in Figure 6. The curve keeps constant in correspondence of branches experiencing no failure. The algorithm seems to have good prediction capabilities: the curve grows slowly at the beginning, i.e., for reliable branches, and fast at the end. Regarding the more reliable branches, we note that out of 1485 failures, there were only 21 in the first 1000, 51 in the first 2000 and 133 in the first 3000. In contrast, for the less reliable branches, there were 144 failures in the 50 most critical branches, i.e., some branches failed multiple times, 224 in the last 100, 590 in the last 500, and 825 in the last 1000. Overall, the model seems capable of capturing the order of criticality of the various branches.

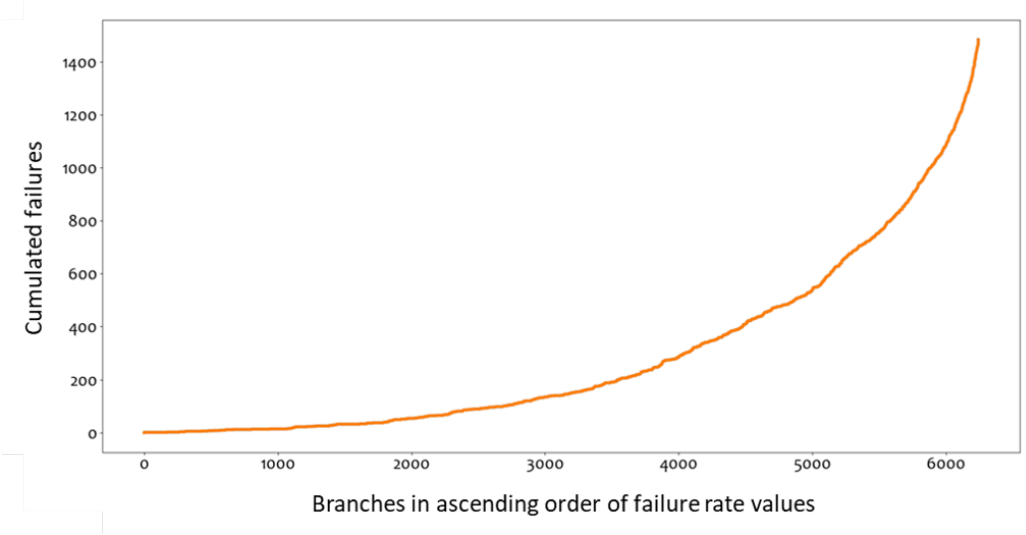

Figure 6: Cumulative failures for the considered network branches.

5.3. Renovation plan

The algorithm presented in Section 4 identified $\Gamma = 854$ sections. Figure 7 shows the distribution of sections S_j. There are almost 150 sections with 3 branches only, whereas there are almost 150 sections with $S_j > 10$. To find the rate of occurrence of the double-failure events, we conservatively assumed that the values of all the model parameters are those corresponding to the bound of the 95% confidence interval associated with the largest failure rate: for λ_0 we consider the upper bound; for β_i parameters we consider the lower bounds.

We show the results assuming a value $\mu_m = 1/(52)h^{-1}$ away from the HW, whereas during the HW this increases up to $\mu_m = 1/(12)d^{-1}$, due to the limited availability of crews compared to the number of failures. For confidentiality, these values are different from the actual ones. Figure 8 shows the distribution of the rate of the double-failure events: in more than 50% of the cases, i.e., 486 out of 854, it is smaller than $3 \cdot 10^{-3}y^{-1}$. In the case of the Milano EPDN, 53 sections can be considered for renovation, whose double-failure event is estimated to occur with a frequency larger than $1/50y^{-1}$. Of course, the final selection of the sections to invest on shall consider additional criteria such as the budget, number of customers supplied, sections length, consequences on the traffic circulation, etc. Making this decision within a portfolio decision analysis framework is expected to lead to more

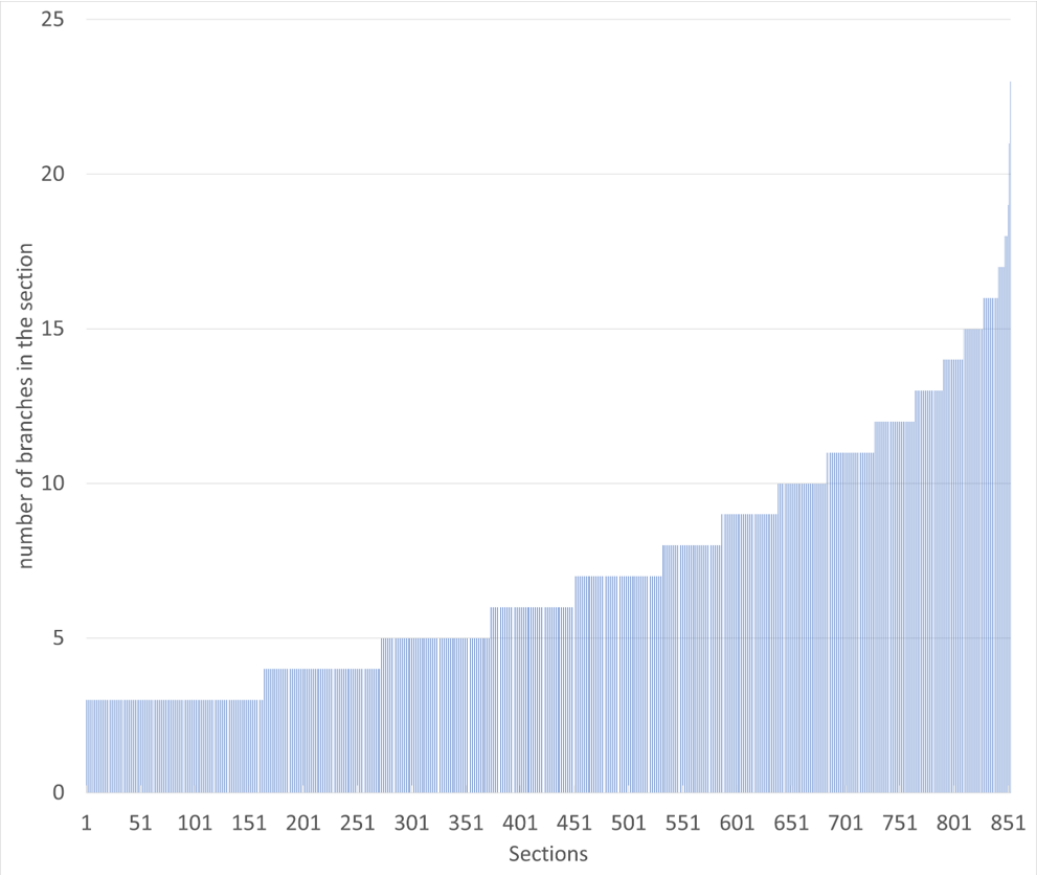

Figure 7: Number of sections and related number of branches therein.

cost-effective plans [60]. This is another issue that will be tackled in future research work, e.g., building on [61].

Two interventions proposed by Unareti in the three-year resilience plan are presented in Figure 9, concerning two sections out of the 53 identified: cable replacement for Section A, in which the branches with largest failure rates are highlighted in yellow, and a new connection for section B.

Cable replacement does not entail topology variation, whereby section A will keep the same extension and serve the same number of customers. With respect to section B, a new connection has been planned in order to decrease both the impact and the probability of double-failure events. The new connection changes from 2 to 3 the degree, i.e., the number of connected edges, of the vertex indicated therein. That is, section B, 7.4 km long, is divided

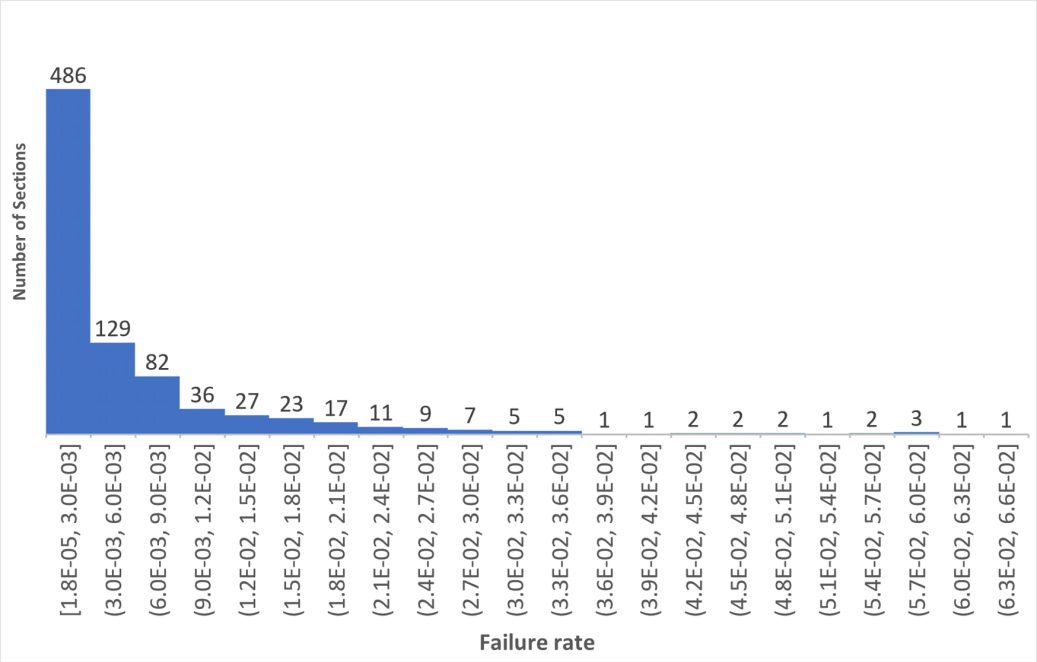

Figure 8: Number of sections and related double-failure events rate of occurrence. In abscissa, we report the intervals of the rate values.

into two subsections of 3,2 km and 4,2 km, respectively. Results of the interventions are summarized in Table 2: these reduce by 80% (section A) and 75% (section B) the current rates of occurrence of the scenarios in which 3213 and 2611 customers, respectively, are disconnected for long times in case of HW.

Table 2: Benefits of including sections A and B in the resilience plan.

Section	Customers	Current length	New length	Current rate	New rate	% rate red.
A	3213	4.4	4.4	0.0224	0.00446	80
B	2611	7.4	3.2 + 4.2	0.02597	0.0067	74

6. Conclusion

We proposed a methodology to identify the most suitable renovation actions to improve the resilience of EPDNs, according to the PBR paradigm issued by the Italian regulator ARERA. The methodology proposes several novel approaches:

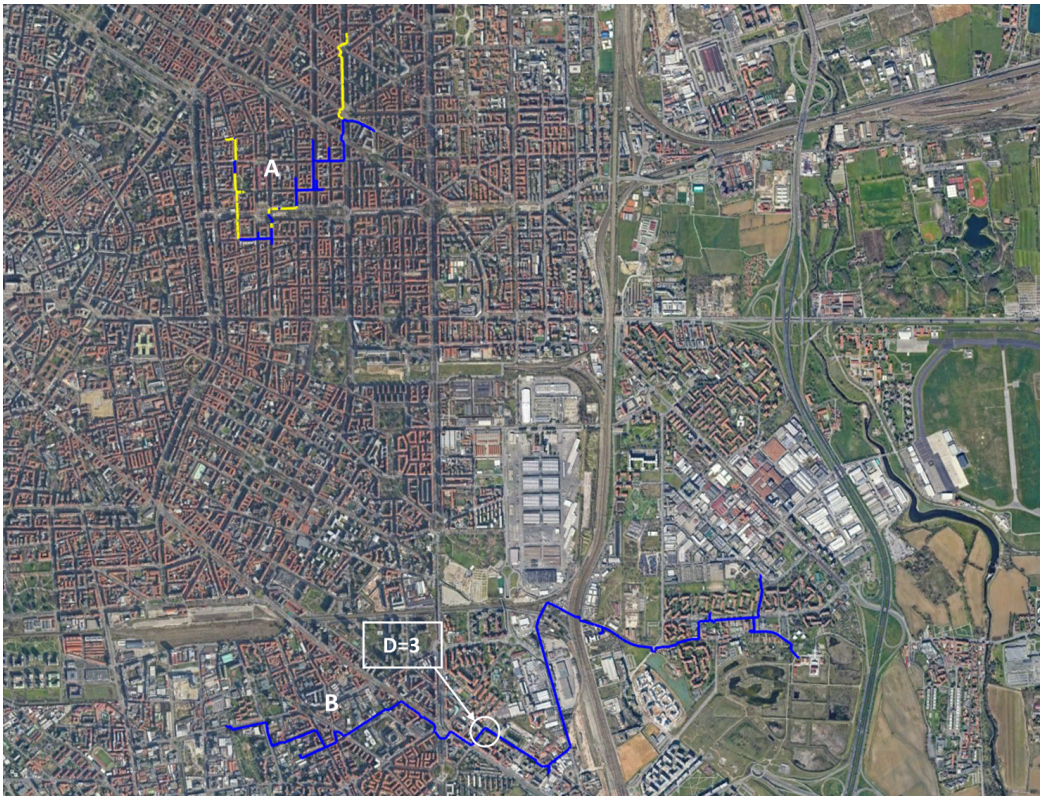

Figure 9: Cables of the sections A and B included in the resilience plan.

- HWs are quantitatively defined through a supervised classification algorithm based on logistic regression with elastic-net penalty to relate temperature, load and humidity data to the heat wave conditions.

- The reliability of the network branches is estimated by fully exploiting the maintenance and operation data typically available for old EPDNs of large cities, which are characterized by lack of registry data, inhomogeneity of component materials and technologies, and variability of operation setting. The developed reliability model encodes the most influencing covariates, which turned out to be the number of failures on the primary substation, the number of joints connecting cables with the same insulation material and the number of joints linking cables with different insulation materials (i.e., XLPE-paper, paper-rubber, rubber-XLPE).

- Finally, the less reliable network sections are identified through a novel combination of a SPP-based algorithm with Markov chain modeling. This approach allows identifying the network sections where a double failure event during a HW period is estimated to occur more frequently than once in 50 year. These events affect the network resilience, whereby renovation actions to reduce the occurrence probability can be submitted to the ARERA for incentives.

The methodology has been applied to the Milano EPDN, giving interesting results and providing valuable insights. Further research work will focus on the definition of metrics to validate the prediction model, the enhancement of the reliability model to give account to the stepwise constant failure rate behavior, the application of optimization models to select the renovation actions, the efficiency improvement of the algorithm to identify the sections.

References

[1] E. D. Vugrin, A. R. Castillo, and C. A. Silva-Monroy, "Resilience metrics for the electric power system: A performance-based approach," *SAND2017-1493 654236, https://doi.org/10.2172/1367499. https://www.osti.gov/servlets/purl/1367499*, 2017.

[2] E. Zio, *An introduction to the basics of reliability and risk analysis*, vol. 13. World scientific, 2007.

[3] A. Ellis, "Microgrids and resilience framework," in *Proc. IRED Symp. Microgrids*, p. 9, 2016.

[4] S. Y. Chung and Y. Xu, "Reliability and resilience in a regulated electricity market: Hong kong under typhoon mangkhut," *Utilities Policy*, vol. 67, p. 101134, 2020.

[5] F. Ciasca, A. Sallati, *et al.*, "Italian national resilience plan 2017: For a more reliable grid," in *2017 AEIT International Annual Conference*, pp. 1–5, IEEE, 2017.

[6] R. R. Billinton and J. R. Acharya, "Major event day segmentation," *IEEE Transactions on Power Systems*, vol. 21, no. 3, pp. 1463–1464, 2006.

[7] E. D. Vugrin, D. E. Warren, M. Ehlen, and R. Camphouse, "A framework for assessing the resilience of infrastructure and economic systems," in *Sustainable and Resilient Critical Infrastructure Systems* (K. Gopalakrishnan and S. Peeta, eds.), 2010.

[8] J.-P. Watson, R. Guttromson, C. Silva-Monroy, R. Jeffers, K. Jones, J. Ellison, C. Rath, J. Gearhart, D. Jones, T. Corbet, C. Hanley, and L. T. Walker, "Conceptual framework for developing resilience metrics for the electricity, oil, and gas sectors in the united states," *SANDIA REPORT*, no. SAND2014-18019.

[9] E. Zio, "The future of risk assessment," *Reliability Engineering and System Safety*, vol. 177, pp. 176–190, 2018.

[10] S. Hosseini, K. Barker, and J. E. Ramirez-Marquez, "A review of definitions and measures of system resilience," *Reliability Engineering & System Safety*, vol. 145, pp. 47 – 61, 2016.

[11] X. Liu, E. Ferrario, and E. Zio, "Identifying resilient-important elements in interdependent critical infrastructures by sensitivity analysis," *Reliability Engineering and System Safety*, vol. 189, pp. 423–434, 2019.

[12] P. Jamborsalamati, M. Moghimi, M. Hossain, S. Taghizadeh, J. Lu, and G. Konstantinou, "A framework for evaluation of power grid resilience case study: 2016 south australian blackout," in *2018 IEEE International Conference on Environment and Electrical Engineering and 2018 IEEE Industrial and Commercial Power Systems Europe (EEEIC/I&CPS Europe)*, pp. 1–6, IEEE, 2018.

[13] D. Luo, Y. Xia, Y. Zeng, C. Li, B. Zhou, H. Yu, and Q. Wu, "Evaluation method of distribution network resilience focusing on critical loads," *IEEE Access*, vol. 6, pp. 61633–61639, 2018.

[14] M. Zare-Bahramabadi, A. Abbaspour, M. Fotuhi-Firuzabad, and M. Moeini-Aghtaie, "Resilience-based framework for switch placement problem in power distribution systems," *IET Generation, Transmission & Distribution*, vol. 12, no. 5, pp. 1223–1230, 2017.

[15] R. Nateghi, "Multi-dimensional infrastructure resilience modeling: an application to hurricane-prone electric power distribution systems," *IEEE Access*, vol. 6, pp. 13478–13489, 2018.

[16] H. Gao, Y. Chen, S. Mei, S. Huang, and Y. Xu, "Resilience-oriented pre-hurricane resource allocation in distribution systems considering electric buses," *Proceedings of the IEEE*, vol. 105, no. 7, pp. 1214–1233, 2017.

[17] N. Zhao, X. Yu, K. Hou, X. Liu, Y. Mu, H. Jia, H. Wang, and H. Wang, "Full-time scale resilience enhancement framework for power transmission system under ice disasters," *International Journal of Electrical Power Energy Systems*, vol. 126, p. 106609, 2021.

[18] M. Amirioun, F. Aminifar, H. Lesani, and M. Shahidehpour, "Metrics and quantitative framework for assessing microgrid resilience against windstorms," *International Journal of Electrical Power Energy Systems*, vol. 104, pp. 716–723, 2019.

[19] I. Abdin, Y.-P. Fang, and E. Zio, "A modeling and optimization framework for power systems design with operational flexibility and resilience against extreme heat waves and drought events," *Renewable and Sustainable Energy Reviews*, vol. 112, pp. 706–719, 2019.

[20] D. E. Sappington, J. P. Pfeifenberger, P. Hanser, and G. N. Basheda, "The state of performance-based regulation in the us electric utility industry," *The Electricity Journal*, vol. 14, no. 8, pp. 71–79, 2001.

[21] L.-M. Perrin, "Mapping power and utilities regulation in europe," *EY Global Power & Utilities Center, EYGM Limited*, 2013.

[22] "Arera - incentivazione economica degli interventi di incremento della resilienza delle reti di distribuzione dell'energia elettrica," 2018.

[23] D. Falabretti, M. Delfanti, and M. Merlo, "Power systems' resilience against ice sleeves: An assessment methodology tested in the smart city vizze project," in *2018 IEEE International Conference on Environment and Electrical Engineering and 2018 IEEE Industrial and Commercial Power Systems Europe (EEEIC/I&CPS Europe)*, pp. 1–6, IEEE, 2018.

[24] UNARETI, "Piano di sviluppo e incremento resilienza," *https://www.unareti.it/unr/unareti/elettricita/ cittadini/piano-di-sviluppo-e-incremento-resilienza/*, 2020.

[25] H. Zou and T. Hastie, "Regularization and variable selection via the elastic net," *Journal of the royal statistical society: series B (statistical methodology)*, vol. 67, no. 2, pp. 301–320, 2005.

[26] I. Goodfellow, Y. Bengio, and A. Courville, *Deep Learning*. MIT Press, 2016.

[27] M. Newby, "Accelerated failure time models for reliability data analysis," *Reliability Engineering & System Safety*, vol. 20, no. 3, pp. 187–197, 1988.

[28] R. K. Ahuja, T. L. Magnanti, and J. B. Orlin, *Network Flows: Theory, Algorithms, and Applications*. Pearson, 2014.

[29] E. Zio, *Computational Methods for Reliability and Risk Analysis*. World Scientific Publishing Company, 2009.

[30] M. Bartos, M. Chester, N. Johnson, B. Gorman, D. Eisenberg, I. Linkov, and M. Bates, "Impacts of rising air temperatures on electric transmission ampacity and peak electricity load in the united states," *Environmental Research Letters*, vol. 11, p. 114008, nov 2016.

[31] J. A. Añel, M. Fernández-González, X. Labandeira, X. López-Otero, and L. De la Torre, "Impact of cold waves and heat waves on the energy production sector," *Atmosphere*, vol. 8, no. 11, 2017.

[32] Y. Zhang, A. Mazza, E. Bompard, E. Roggero, and G. Galofaro, "Data-driven feature description of heat wave effect on distribution system," in *2019 IEEE Milan PowerTech*, pp. 1–6, IEEE, 2019.

[33] D. A. Reynolds, "Gaussian mixture models.," *Encyclopedia of biometrics*, vol. 741, 2009.

[34] C. E. Rasmussen, "The infinite gaussian mixture model," in *Advances in neural information processing systems*, pp. 554–560, 2000.

[35] A. Burkov, *The Hundred-Page Machine Learning Book*. Andriy Burkov, 2019.

[36] F. Pedregosa, G. Varoquaux, A. Gramfort, V. Michel, B. Thirion, O. Grisel, M. Blondel, P. Prettenhofer, R. Weiss, V. Dubourg, *et al.*,

"Scikit-learn: Machine learning in python," *Journal of machine learning research*, vol. 12, no. Oct, pp. 2825–2830, 2011.

[37] N. Schwertman, M. Owens, and R. Adnan, "A simple more general boxplot method for identifying outliers," *Computational Statistics and Data Analysis*, vol. 47, no. 1, pp. 165–174, 2004.

[38] F. Pedregosa, G. Varoquaux, A. Gramfort, V. Michel, B. Thirion, O. Grisel, M. Blondel, P. Prettenhofer, R. Weiss, V. Dubourg, J. Vanderplas, A. Passos, D. Cournapeau, M. Brucher, M. Perrot, and E. Duchesnay, "Scikit-learn: Machine learning in Python," *Journal of Machine Learning Research*, vol. 12, pp. 2825–2830, 2011.

[39] R. A. Johnson, D. W. Wichern, *et al.*, *Applied multivariate statistical analysis*, vol. 5. Prentice hall Upper Saddle River, NJ, 2002.

[40] B. Schlkopf, A. J. Smola, and F. Bach, *Learning with kernels: support vector machines, regularization, optimization, and beyond*. the MIT Press, 2018.

[41] V. Svetnik, A. Liaw, C. Tong, J. C. Culberson, R. P. Sheridan, and B. P. Feuston, "Random forest: a classification and regression tool for compound classification and qsar modeling," *Journal of chemical information and computer sciences*, vol. 43, no. 6, pp. 1947–1958, 2003.

[42] M. A. Nielsen, *Neural networks and deep learning*, vol. 2018. Determination press San Francisco, CA, 2015.

[43] H. M. Nemati, A. Sant'Anna, S. Nowaczyk, J. H. Jürgensen, and P. Hilber, "Reliability evaluation of power cables considering the restoration characteristic," *International Journal of Electrical Power & Energy Systems*, vol. 105, pp. 622–631, 2019.

[44] D. Johnson, D. W. Coit, R. Kosaka, and K. Megow, "System level reliability analyses and predictions in a varying stress environment," in *2013 Proceedings Annual Reliability and Maintainability Symposium (RAMS)*, pp. 1–6, 2013.

[45] X. Zhang and E. Gockenbach, "Component reliability modeling of distribution systems based on the evaluation of failure statistics," *IEEE Transactions on Dielectrics and Electrical Insulation*, vol. 14, 2007.

[46] M. Gilvanejad, H. A. Abyaneh, and K. Mazlumi, "A three-level temperature curve for power cables aging failure rate estimation incorporating load cycling," *International Transactions on Electrical Energy Systems*, vol. 23, no. 6, pp. 853–866, 2013.

[47] B. Hennuy, F. Steennis, B. Aerns, P. Oosterlee, P. Leemans, P. Soepboer, T. Van Rijn, R. Meier, E. De Ridder, H. Grandjean, M. Van Den Berg, P. Buys, and L. Bokma, "Measurement of the force induced by thermal expansion of conductor of mv cables and impact on mv joints," vol. 2013, 2013.

[48] W.-Z. Chang, F. Du, J.-G. Bi, S. Yuan, Y.-P. Gong, and Y. Yang, "Assessment of creeping discharge initiated by metal particles on the silicone rubber/XLPE interface in cable joints," *Journal of Electrical Engineering*, vol. 70, pp. 370–378, Sept. 2019.

[49] S. Powell, A. Ivanova, and D. P. Chassin, "Fast solutions in power system simulation through coupling with data-driven power flow models for voltage estimation," *CoRR*, vol. abs/2001.01714, 2020.

[50] L. Buechler, "Learning power flow mappings for power grid simulation," *CS230: Deep Learning, Winter 2018, Stanford University, CA, http://cs230.stanford.edu/projects_winter_2020/reports/32107581.pdf.*

[51] S. Derksen and H. J. Keselman, "Backward, forward and stepwise automated subset selection algorithms: Frequency of obtaining authentic and noise variables," *British Journal of Mathematical and Statistical Psychology*, vol. 45, no. 2, pp. 265–282, 1992.

[52] E. Wagenmakers and S. Farrell, *AIC model selection using Akaike weights*, pp. 192–196. Psychonomic Bulletin and Review, Psychonomic Society, 2004.

[53] S. Chiappa, "Explicit-duration markov switching models," *arXiv preprint arXiv:1909.05800*, 2019.

[54] A. Bosisio, A. Berizzi, C. Bovo, E. Amaldi, and S. Fratti, "Gis-based urban distribution networks planning with 2-step ladder topology considering electric power cable joints," in *2018 AEIT International Annual Conference*, pp. 1–6, 2018.

[55] A. Bosisio, E. Amaldi, A. Berizzi, C. Bovo, and S. Fratti, "A milp approach to plan an electric urban distribution network with an h-shaped layout," in *2015 IEEE Eindhoven PowerTech*, pp. 1–5, 2015.

[56] E. Volodin and A. Y. Yurova, "Summer temperature standard deviation, skewness and strong positive temperature anomalies in the present day climate and under global warming conditions," *Climate dynamics*, vol. 40, no. 5-6, pp. 1387–1398, 2013.

[57] ARPA, "Meteorological data of Milan," *https://www.arpalombardia.it*, 2020.

[58] V. C. Raykar, H. Steck, B. Krishnapuram, C. Dehing-Oberije, and P. Lambin, "On ranking in survival analysis: Bounds on the concordance index," in *Proceedings of the 20th International Conference on Neural Information Processing Systems*, NIPS'07, (Red Hook, NY, USA), p. 1209–1216, Curran Associates Inc., 2007.

[59] A. R. Brentnall and J. Cuzick, "Use of the concordance index for predictors of censored survival data," *Statistical Methods in Medical Research*, vol. 27, no. 8, pp. 2359–2373, 2018. PMID: 27920368.

[60] J. Liesiö, A. Salo, J. Keisler, and A. Morton, "Portfolio decision analysis: Recent developments and future prospects," *European Journal of Operational Research*, vol. 293, no. 3, pp. 811–825, 2021.

[61] A. Mancuso, M. Compare, A. Salo, and E. Zio, "Portfolio optimization of safety measures for reducing risks in nuclear systems," *Reliability Engineering and System Safety*, vol. 167, pp. 20–29, 2017.

Appendix A. Pseudocode

The algorithm considers all the nodes with at least three branches (lines 9-11) and identifies the sections γ_j as the shortest paths towards the nodes of degree larger than 3 or to the HV/MV substations.
Functions *node*() and *arc*() (e.g., line 16), return the IDs of the nodes and arcs, respectively, of the input path.
Function Reduce allows eliminating the single branches like that from node 3 to 2 in Figure 1. These are encoded in node 2 through arrays V_2 and E_2.
Notice that the algorithm does not consider the direct links among HV/MV substations. These have been excluded from the overall analysis, due to the very different operating conditions.
Finally, the efficiency of the algorithm can be improved. This will be done in future research work.

Algorithm 1 Section Identification

Build graph $\mathcal{G} = (V, E)$ from the network shape file ▷ $V = \{1, ..., \nu\}$, $E = \{1, ..., B\}$
Identify set $P \subset V$ of HV/MV substations
stop := False
for all $i \in V$ **do**
    $V_i \leftarrow i$; $E_i \leftarrow \emptyset$ ▷ V_i and E_i =sets of nodes and arcs, respectively, associated to each node
while *stop*=False **do**
    $(\mathcal{G}, stop) = \text{Reduce}(\mathcal{G})$ ▷ see Function below
$j \leftarrow 0$
$A \leftarrow \text{adj}(\mathcal{G})$ ▷ Build the adjacency matrix [28]
$v \leftarrow \text{sumcolumn}(A)$ ▷ sum over the A columns
$X_2 \leftarrow \text{find}(v \geq 3) \setminus P$
while $X_2 \neq \emptyset$ **do**
    Select i from X_2
    $\mathcal{D} = SPP(\mathcal{G}, i, P \cup X_2 \setminus i)$ ▷ set of shortest sub-graphs connecting i to all nodes in X_2 and P
    for all $d \in \mathcal{D}$ **do**
        $N_d \leftarrow node(d)$; $Y_d \leftarrow arc(d)$ ▷ identification of nodes and arcs of path d
        if $|N_d \cap (X_2 \cup P)| = 2$ **then** ▷ Select paths including no more than 1 node of X_2 and P
            $j \leftarrow j + 1$
            $N \leftarrow \bigcup_{\nu \in N_d} V_\nu \cup N_d$; $Y \leftarrow \bigcup_{\nu \in Y_d} E_\nu \cup Y_d$;
            $\gamma_j = (N, Y)$ ▷ Graph identifying the section
        $n = N \cap (X_2 \cup P) \setminus i$
        $node(\mathcal{G}) \leftarrow (node(\mathcal{G}) \setminus N) \cup n$
        $arc(\mathcal{G}) \leftarrow arc(\mathcal{G}) \setminus Y$
    $A \leftarrow \text{adj}(\mathcal{G})$
    $v \leftarrow \text{sumcolumn}(A)$
    $X_2 \leftarrow \text{find}(v \geq 3) \setminus P$

Algorithm 2 Graph Reduction

function REDUCE($\mathcal{G}$)
  $A = \text{adj}(\mathcal{G})$
  $v \leftarrow \text{sumcolumn}(A)$
  $X_1 \leftarrow \text{find}(v = 1) \setminus P$ ▷ leaf nodes ≠ busbars and HV/MV substations
  if $X_1 \neq \emptyset$ **then**
    Select i from X_1
    $j \leftarrow A(i, :) = 1$ ▷ find the connected node
    $V_j \leftarrow V_j \cup i \cup V_i$
    $E_j \leftarrow E_j \cup (i, j) \cup E_i$ ▷ append sub-graph of node i to that of j
    $node(\mathcal{G}) \leftarrow node(\mathcal{G}) \setminus i$
    $arc(\mathcal{G}) \leftarrow arc(\mathcal{G}) \setminus (i, j)$ ▷ remove node i and arc (i, j) from the graph
    $stop \leftarrow$ False
  else
    $stop \leftarrow$ True
  return $(\mathcal{G}, stop)$